

See discussions, stats, and author profiles for this publication at: <https://www.researchgate.net/publication/231686539>

Interphase Morphology of Liquid Crystalline Polymer/Glass Fiber Composites: Effect of Fiber Surface Treatment

ARTICLE *in* MACROMOLECULES · OCTOBER 1994

Impact Factor: 5.8 · DOI: 10.1021/ma00100a046

CITATIONS

6

READS

12

3 AUTHORS, INCLUDING:



An-Chung Su

National Tsing Hua University

96 PUBLICATIONS 1,966 CITATIONS

SEE PROFILE

Interphase Morphology of Liquid Crystalline Polymer/Glass Fiber Composites: Effect of Fiber Surface Treatment

Wun-Gue Lee, Tzu-Chien J. Hsu,* and An Chung Su

Institute of Materials Science and Engineering, National Sun Yat-Sen University, Kaohsiung, Taiwan 804, Republic of China

Received May 25, 1994; Revised Manuscript Received July 18, 1994*

ABSTRACT: The effect of surface treatment on the interphase morphology of liquid crystalline copolyester/glass fiber (LCP/GF) composites has been investigated by polarized light microscopy (PLM), scanning electron microscopy (SEM), differential scanning calorimetry (DSC), and wide-angle X-ray diffractometry (WAXD). The main objective of this study was to identify the role of fiber in the formation of microstructure and morphology of the composites, particularly its influence on the anisotropic nature of LCP. Two coupling agents, γ -methacrylate propyltrimethoxysilane (γ -MPS) and phenyltriethoxysilane (PTS), were employed for the surface treatment of GF. The former reacted with the LCP, the latter did not. "Model composites" were prepared by embedding a single glass fiber in the LCP melt under mechanical shearing between glass slides at elevated temperatures. Experimental results from PLM and SEM revealed a parallel-to-GF LCP orientation at the interface for the composite with no coupling agent, a perpendicular-to-GF LCP orientation for the composite with γ -MPS, and a random LCP orientation for the composite with PTS. Factors affecting the formation of these interphase morphologies were analyzed; these factors included (1) the mechanical shearing, (2) the guiding, anchoring, and packing effects of GF, and (3) the interfacial modification by γ -MPS due to the occurrence of transesterification. The relative importance of the above factors was compared. The above effects of GF were confirmed by comparing the as-sheared and the annealed LCP composites. The occurrence of transesterification was further supported by DSC data which showed a low-temperature transition peak at 224 °C in addition to the k-n transition peak. WAXD results indicated almost no change of LCP crystalline structure in the presence of coupling agent, possibly due to the large difference in molecular size of the LCP and coupling agent.

Introduction

Thermotropic liquid crystalline polymers (LCPs) have long been considered as one of the high-performance engineering thermoplastics. The unique nematic structure at the melt state is due mainly to their rigid rod, the rigidity being conferred by the aromatic repeating units and ester linkages. These render themselves with excellent processibility, high-temperature stability, and strong chemical resistance.¹ When blended with other thermoplastics such as poly(ether ether ketone), poly(ethylene terephthalate), polycarbonate, and polyethylene, a molecular composite or in-situ composite can be achieved. The composite is also self-reinforced by the rigid-rod configuration of LCP. In other cases, LCP is used as a processing aid due to its relatively low melt viscosity at the nematic state. In general, technological applications of LCPs depend strongly on the capability to control their microscopic structure during processing. This is especially true in the LCP composites in which short fibers or fillers are added. These types of composites, which are targeted to improve the mechanical and thermal properties of neat LCPs, have found commercial applications in recent years. However, one has to caution that the presence of fibers in the LCP composites might affect the unique anisotropic property of LCPs in a macroscopic scale and the interphase morphology in a microscopic scale.

Although research on the phase transition, rheology, and crystallinity of neat LCPs has met with great success during the last decade, little effort has been directed toward the understanding of the LCP composites, especially at the fiber-LCP interphase and interface. A limited number of studies have been devoted to the LCP/fiber composites on the mechanical properties. Chung and McMahon

developed a continuous carbon fiber-reinforced LCP (LCP/CF) prepreg tape by a melt impregnation method.² The resultant laminates showed better impact resistance and thermal retention than the epoxy/CF composites, but poor compression and shear strength. Poor interfacial adhesion between the matrix and fiber was the major cause.

According to Voss and Friederich,³ the tensile strength and fracture toughness of short glass fiber/LCP (LCP/GF) composites were lower than those of neat LCP. They attributed this to the debonding at the interphase due to poor adhesion. The microstructure of LCP molecules at and near the interphase, which might be an important site for stress transfer, was not considered in their study. The influence of short glass fiber reinforcement on the mechanical anisotropy of injection-molded LCP composites has been investigated by Chivers and Moore.⁴ They reported a reduction of anisotropy in in-plane stiffness and fracture toughness. In addition, the glass fibers disrupted the LCP orientation to some extent. No detailed experimental proofs were provided. In general, it is believed that the interaction between fiber and LCP, the orientation of fiber and LCP, and the fiber content may all have a significant effect on the mechanical properties of the LCP composites.

To improve the adhesion of the LCP/CF composite, King et al. applied amine type coupling agents to the surface of PAN-based CF.⁵ They reported an increase of 10–20% in the short beam shear strength compared to the untreated composite. Their ESCA and FTIR analyses suggested the existence of chemical interactions with functional groups on the fiber surface. SEM analyses of the failure surface showed that failure occurred in the LCP matrix, indicating a strong fiber–matrix adhesion. Various electrochemical surface treatments of CF were also applied to the same LCP/CF composites by King et al.⁶ The composite with CF treated by an electrochemically polymerized coating of poly(phenylene oxide) showed

* To whom the correspondence should be addressed.

Abstract published in *Advance ACS Abstracts*, September 15, 1994.

an enhanced shear strength by 14% compared to the untreated composite.

The molecular orientation of LCP in the LCP/CF composites has been investigated by Bhama and Stupp.⁷ They applied polarized light microscopy to analyze the interfacial zone in the composite samples and broadband proton nuclear magnetic resonance to measure the rate of magnetic alignment of molecules in the matrix and near the CF surface. Results indicated that the orientation and orientation dynamics of the LCP matrix were strongly influenced by the fiber surfaces. The nematic ordering of LCP was stabilized as the composite was heated toward complete isotropization. Bhama and Stupp attributed this to the development of zones around the fibers with a common molecular orientation anchored by the CF surface. In another study of the mechanism of surface-induced alignment of nematic liquid crystals (LCs), Creagh and Kmetz have found that under an electric field normal to the substrate surface, quiescent alignment of LC was determined by the physical interaction of the LCs with the substrates.⁸ If the substrate was of low surface energy, the alignment of LC was homeotropic. If the substrate was of high surface energy with proper chemical nature, the orientation of LCs was locally homogeneous. Furthermore, if the high surface energy substrate possessed long range order (such as fibers), the LCs assumed uniformly homogeneous alignment. Shen et al. emphasized the formation of the LC molecular monolayers through a molecular epitaxy mechanism in order to minimize the elastic energy of LCs.⁹ This resulted in a surface-induced bulk alignment to give a long range order.

Understanding the role of fiber in the LCP composites is far from completion. Most of the research work mentioned above concentrated on the mechanical properties only. The main objective of this work is to identify the influence of glass fiber on the microstructure and morphology of the LCP, with a major emphasis on the interphase between the LCP and fiber. To control the surface quality of the glass fiber, we have selectively chosen two coupling agents, γ -methacrylate propyltrimethoxysilane (γ -MPS) and phenyltriethoxysilane (PTS). While both can react with glass fibers, only the former is expected to react with the LCP, not the latter. Comparisons between the effect of surface-treated and untreated glass fibers on the interphase morphology are made and the possible reasons proposed. These coupling agents have been used to study the effect of surface treatment of particulates (glass beads) on the curing kinetics of unsaturated polyester resin by differential scanning calorimetry and to estimate quantitatively the effect of these coupling agents by applying a free radical kinetic model.¹⁰ It was found that the resin with treated particulates generally showed a faster reaction rate and conversion than the resin with untreated particulates and that no obvious difference on the curing kinetics was observed between these two coupling agents.

Experimental Section

1. Materials. The LCP used (Vectra-A950, Celanese Co.) in this study contained 70 mol % 4-hydroxybenzoic acid (HBA) and 30 mol % of 6-hydroxy-2-naphthoic acid (HNA). According to the supplier, this main-chain LCP has an intrinsic viscosity of 5 dL/g (at 60 °C in the solvent pentafluorophenol), a number average molecular weight of ca. 30 000, and a density of 1.4 g/cm³. Its melting temperature is ca. 280 °C (by DSC), and the decomposition temperature is ca. 490 °C (by TGA). All LCPs were vacuum dried at 100 °C for 12 h before use. Type E glass fiber was used with density 2.54 g/cm³ and an average length and diameter of ca. 300 and 9 μ m, respectively (aspect ratio = 33).

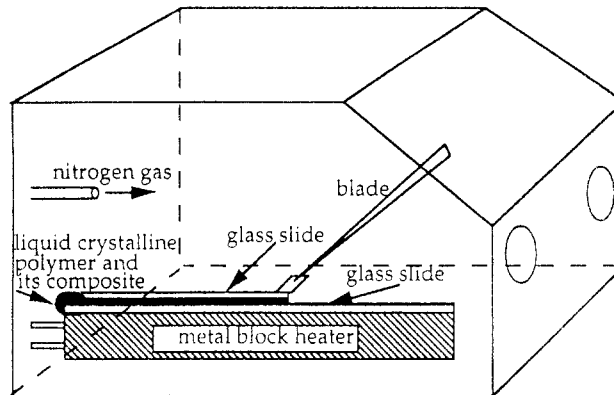


Figure 1. Schematic illustrating the preparation of sheared films of LCPs and LCP composites.

The glass fibers were heated in an oven at 600 °C for 3 h to remove any possible existing sizing agent. After heating, the glass fibers were cooled to room temperature for 120 h to restore the Si-OH bonds on the glass fiber surface. Two types of silane coupling agent were used (Janssen Chemical): γ -methacrylate propyltrimethoxysilane (γ -MPS) and phenyltriethoxysilane (PTS). Both coupling agents were used as received.

2. Surface Treatment of Glass Fiber. An aqueous solution of the coupling agent (γ -MPS and PTS, with 0.1 wt %) was prepared at room temperature using deionized water. After thorough mixing, the solution was kept at room temperature for 30 min to facilitate the following hydrolysis: $R'-SiX_3 + 3H_2O \rightarrow R'Si(OH)_3 + 3HX$ where X represents $-OCH_3$ in γ -MPS and $-OC_2H_5$ in PTS and R' is the corresponding component in the respective coupling agent. The glass fibers were then mixed with an equal amount by weight of the aqueous solution for 3 min by means of a mechanical stirrer, and the solution was then suctioned. At this stage, both γ -MPS and PTS reacted with the Si-OH bonds on the surface of the glass fiber to form the Si-O-Si bondings.¹⁰ The treated glass fibers were then dried at 90 °C for 90 min and later stored in a vacuum chamber of 20% relative humidity before mixing with LCP.

3. Sample Preparation. Neat LCP samples were first heated at 320 °C (40 deg above its melting temperature) for 10 min to destroy any possible crystallites and to remove any previous thermal-mechanical history. They were then quenched in the air. A slice of LCP sample was cut from the pellet and placed on a glass slide at 320 °C for 10 min; then a single glass fiber (with or without the coupling agent treated) was put on top of the LCP sample. Another glass slide was further put on the top of the glass fibers. These samples were sheared by pushing the top glass slide with a metal blade, as illustrated in Figure 1. Then a thin film of "model composite" with a thickness of 5 μ m (for PLM) or 0.2 mm (for SEM) was obtained. One can estimate the shear rate $\gamma = \Delta v / \Delta y$ by recording the final film thickness Δy and the velocity Δv ($\Delta v = \Delta x / \Delta t$, the time Δt elapsed for pushing the metal blade for a distance of Δx). Thus two shear rates were applied; the low shear rate was ca. 20 s⁻¹ and the high shear rate was ca. 100 s⁻¹. The model composite was then quickly cooled (ca. 300 °C/min) to room temperature in order to preserve its morphology at the elevated temperature. For the purpose of comparison, the sheared films were further reheated at 320 °C for 1 h and then slowly cooled at 20 °C/min to room temperature. Table 1 lists the materials used in this study and the sample designations.

4. Sample Characterization. For polarizing light microscopy (PLM, Nikon Optiphoto-pol), the sheared sample was positioned so that either the polarizer or analyzer of PLM was parallel to the shearing direction. Optical morphology was obtained at room temperature. For scanning electron microscopy (SEM, Jeol LSM-35CF), the sheared sample was etched with 98% concentrated sulfuric acid at 40 °C for 40 min. This allowed removal of the amorphous phase and some possible low molecular weight residuals in the LCP. Thus, better topology could be obtained by SEM observation. The secondary electron image was adopted at 25 kV. The SEM sample was also prepared by fracturing the sheared sample under liquid nitrogen temperature. The fractured surface was then gold-coated.

Table 1. Sample Designations in This Study^a

sample code	ingredients		
	LCP	fiber	coupling agent
LCP	BN		
LCP/ γ -MPS	BN		γ -MPS
LCP/PTS	BN		PTS
LCP/GF	BN	glass fiber	
LCP/GF/ γ -MPS	BN	glass fiber	γ -MPS
LCP/GF/PTS	BN	glass fiber	PTS

^a BN: neat liquid crystalline polymer = 70 mol % 4-hydroxybenzoic acid (HBA) + 30 mol % 6-hydroxy-2-naphthoic acid (HNA). γ -MPS: γ -methacrylate propyltrimethoxy silane. PTS: phenyltriethoxysilane.

For differential scanning calorimetry (DSC, DuPont 9900), the neat LCP samples were sheared under a high shear rate with the same shearing condition as the model composites. It was then finely chopped and thoroughly mixed with coupling agent at 50 wt %, without the interference from GF. Comparisons among the neat LCP, the neat coupling agent, and the blend LCP/coupling agent were then made.

All the DSC samples were first scanned from 25 to 320 °C at a heating rate of 20 °C/min. Then the samples were quenched (ca. 300 °C/min), followed by a second scan which was also from 25 to 320 °C at a heating rate of 20 °C/min. DSC samples after the second scan were further analyzed by wide-angle X-ray diffraction (WAXD, Siemens D 5000), using the Ni-filtered Cu K α radiation (40 kV, 30 mA, with wavelength 1.5418 Å). The WAXD sample was positioned with the shear direction perpendicular to the X-ray incident beam. The X-ray angle varied from 10 to 45° at a scanning rate of 1°/min.

Results

Composites with Untreated Glass Fibers. Figure 2 shows the morphology of LCP/GF composites with untreated GF by polarized light microscopy. Under a high shear rate (Figure 2a), a thin layer of LCP with a banded optical texture ca. 10 μ m wide, *perpendicular* to the glass fiber (or the shear direction), can be identified. The banded texture, as well as the tight texture (see below), was previously described by Viney et al. to indicate the molecular orientation and microstructure of sheared thermotropic copolymers.¹¹ The same observation prevails for the same sample under a low shear rate (Figure 2b), but in a less orderly pattern, i.e., the tight texture. The corresponding SEM micrographs are presented in Figure 3, where samples were etched in 98% sulfuric acid. Under a high shear rate, the LCP molecules near the GF surface now are *parallel* to the glass fiber (Figure 3a). Sample LCP/GF under low shear rate exhibits less ordered interphase morphology (Figure 3b).

It is well established that in the liquid crystalline phase, the LCP molecules arrange themselves in a regular fashion to form domains with few discontinuous defects.^{12,13} The formation of the banded structure results from a high degree of register of the LCP molecules between and within the layers;¹⁴ it is the consequence of a periodic variation in the orientation of the principal optical vibration direction about the shear axis, due primarily to the corresponding variation in the direction of the long axis of the twisted fibrillar structure of LCP molecules. Therefore, the actual orientation of these LCP domains is just 90°, which is different from what is observed under PLM. In other words, the LCP molecules are actually parallel to the direction of the glass fiber, as observed from SEM. This "opposite" result has also been confirmed by several other researchers.¹⁴⁻²⁰ Note that no transcrystallinity, where the crystalline polymer near the GF surface is grown perpendicular to GF, is observed for the LCP composite system in this study. The transcrystallinity

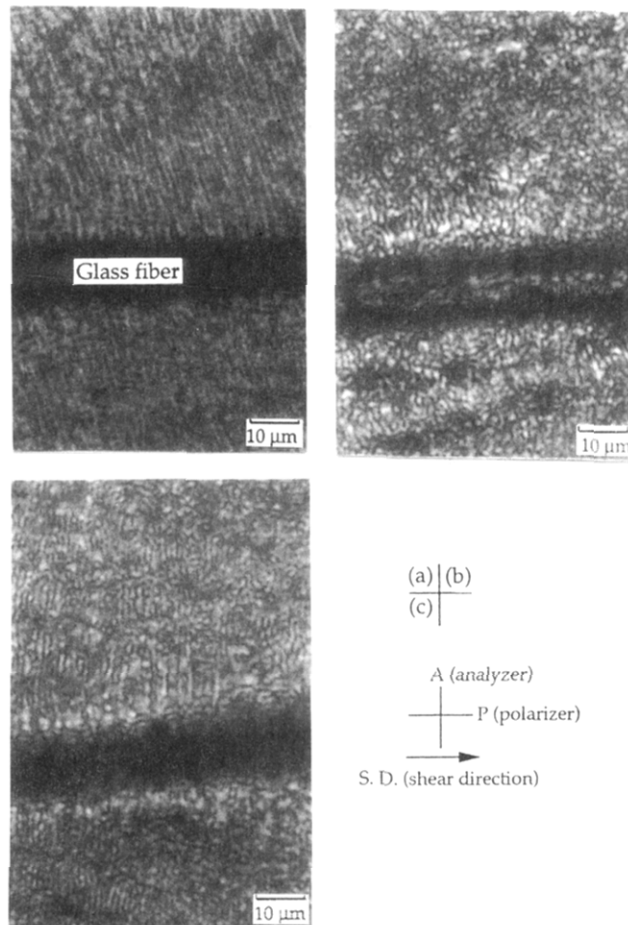


Figure 2. Polarized light micrographs of sheared films of sample LCP/GF prepared under (a) a high shear rate, (b) a low shear rate, and (c) a high shear rate and after annealing.

has been identified in the non-LCP composites such as polypropylene and poly(ether ether ketone) systems by others.

The effect of shearing can further be identified when one examines the texture of LCP molecules away from the glass fiber. A tight optical texture with no regular pattern of LCP is found for sample LCP/GF under a low shear rate.¹¹ On the other hand, the sample under a high shear rate still maintains the banded texture (Figure 2). This demonstrates that the microstructure of LCPs can easily be controlled during processing, due primarily to its relatively low viscosity at the nematic state.

Figure 2c is the micrograph showing the shear film of LCP/GF under a high shear subjected to a thermal annealing at 320 °C for 60 min and then slowly cooled to room temperature at 20 °C/min. It is found that the banded texture near the glass fiber remains the same, while LCP molecules away from the glass fiber surface change from the banded to the tight texture. The same observation is found in the corresponding SEM micrograph (Figure 3c) where the annealed LCP molecules remain parallel to GF.

Unlike the two-phase polymer blends where one of the phases can easily be removed by a selective organic solvent, the removal of the amorphous portion by the concentration sulfuric acid from LCP is relatively difficult, depending strongly on the extent of etching. This is the major reason why the SEM micrographs of LCP composites in this study appear nominally somewhat different. With the same etching time, the annealed LCP composite in Figure 3c appears to be less clear than the as-sheared samples, but

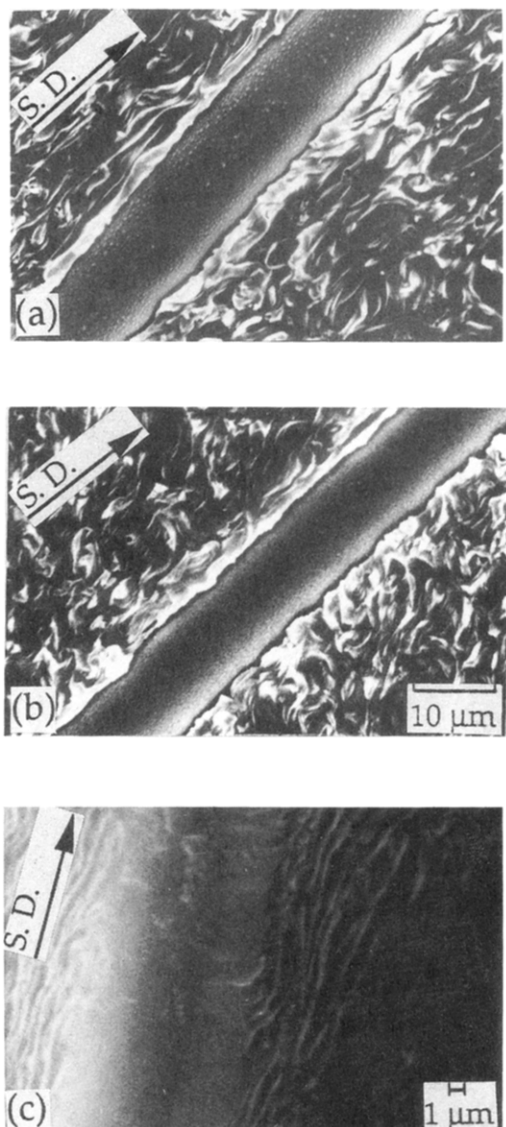


Figure 3. Scanning electron micrographs of sheared films of sample LCP/GF prepared under (a) a high shear rate, (b) a low shear rate, and (c) a high shear rate and after annealing. Samples were etched in 98% sulfuric acid for 40 min.

its morphology can still be identified. In addition, the inherent nature of SEM prohibits the identification of the interphase, especially the banded texture as observed by PLM. However, SEM provides the "real" morphology of the LCP composite which is complementary to the optical image observed by PLM.

Composites with Coupling Agent-Treated Glass Fibers. Under the same shearing conditions, sample LCP/GF/ γ -MPS under a high shear rate exhibits an optical texture completely different from sample LCP/GF. PLM shown in Figure 4a clearly indicates that a thin layer of LCP molecules (ca. 10–20 μm wide) near GF appears parallel to the glass fiber, while LCP molecules farther away from GF appear perpendicular to the glass fiber; both have banded texture. Reducing the shear rate does not alter the optical morphology of LCP molecules near GF, as indicated in Figure 4b, although the microstructure of LCP molecules farther away from GF appears to be somewhat less banded. Upon annealing at 320 °C for 60 min, Figure 4c,d reveal that the morphology of LCP molecules near GF is retained, while LCP molecules farther away from GF have changed from banded to tight optical texture. Clearly, all the thermal or mechanical history of

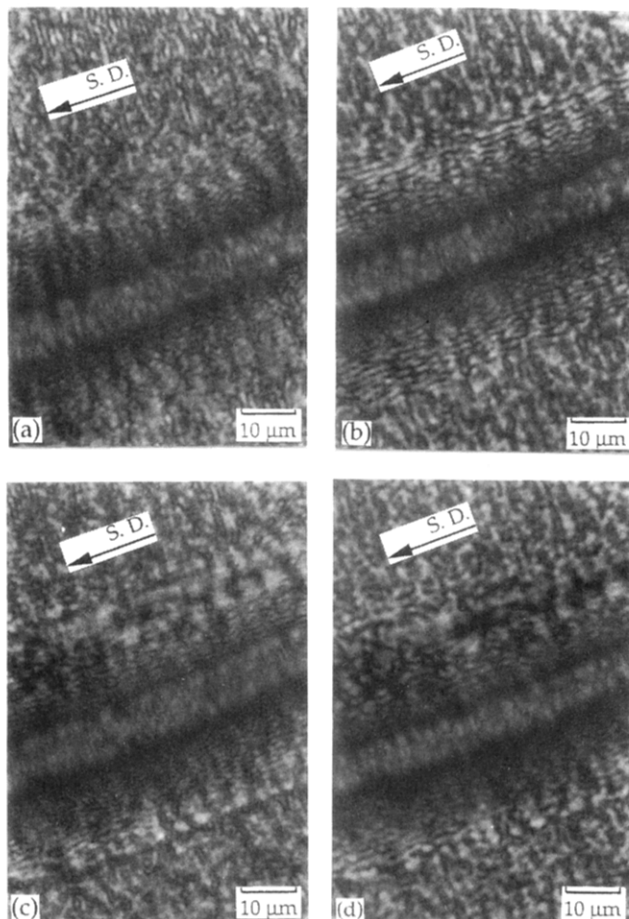


Figure 4. Polarized light micrographs of sheared films of sample LCP/GF/ γ -MPS prepared under (a) a high shear rate, (b) a low shear rate, (c) a high shear rate and after annealing, (d) a low shear rate and after annealing.

LCP molecules farther away from GF is removed by annealing. The coupling agent γ -MPS definitely plays an important role in determining the interphase morphology.

For sample LCP/GF/PTS, the PLM shown in Figure 5b indicates a loose or random arrangement of LCP molecules (ca. 5 μm wide) near the glass fiber. It is even less orderly than those LCP molecules farther away from GF (Figure 5a). Note that a clear interphase boundary can still be identified. In this case, the mechanical shearing cannot force the LCP molecules near the GF to arrange themselves in a regular fashion. With no doubt, the role of coupling agent PTS is quite different from that of γ -MPS.

Figure 6 shows the SEM micrographs of the cryogenically fractured surface of LCP composites with and without silane coupling agents. It is seen that the composite with γ -MPS (Figure 6b) shows excellent retention of the alignment of LCP molecules on the GF surface, indicating a strong adhesive bonding; whereas the composite with PTS (Figure 6c) shows a clean, debonded GF surface, with barely no LCPs attached. It is interesting to note that the adhesion of the composite without the coupling agent (Figure 6a) is better than the composite with the PTS coupling agent. The improvement of adhesion between GF and LCPs in the composite with γ -MPS must have resulted from interfacial modification brought about by the coupling agent. Summarized in Table 2 are the results of experimentally observed interphase morphology.

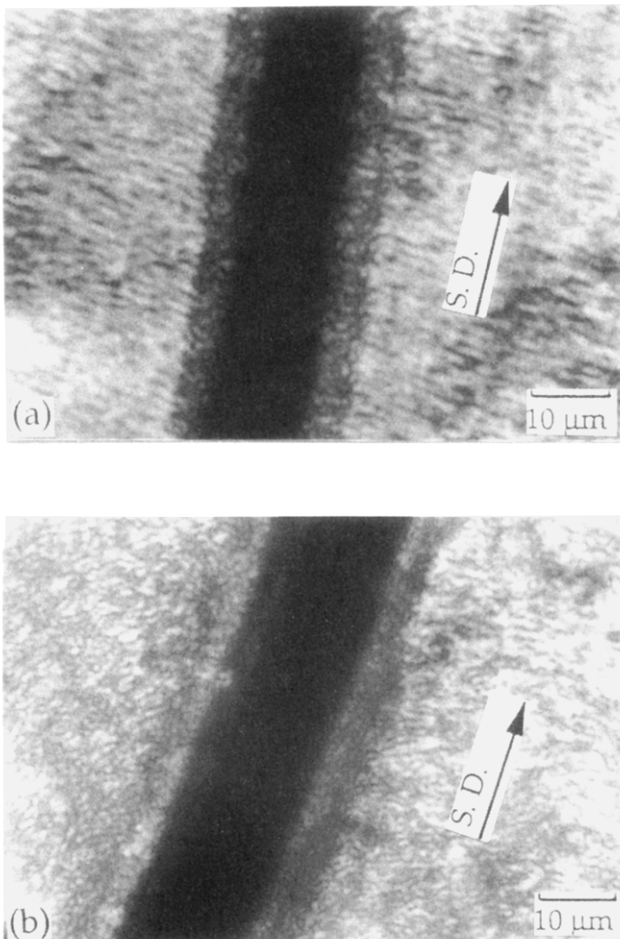


Figure 5. Polarized light micrographs of sheared films of sample LCP/GF/PTS prepared under (a) a high shear rate and (b) a low shear rate.

Discussion

Formation of Interphase Morphology. For sample LCP/GF, the interphase morphology is mainly controlled by the flow field around GF in a shearing flow. Because of the extremely low shear viscosity, the nematic LCPs are easily deformed and then rearrange themselves parallel (by SEM) to GF, which is also positioned parallel to the shear direction. Under the mechanical shearing force, the untreated GF helps not only to *guide* the LCP molecules but also to *anchor* the LCP molecules by its coarse surface, allowing a more compact structure of LCP molecules near the GF surface. Thus, an additional *packing* effect of the GF may be assumed. The coarse GF surface also offers potential opportunity for mechanical locking between the GF and the LCPs. The guiding, anchoring, and packing effects provided by the glass fiber on the interphase morphology are even greater than the effect brought about from the mechanical shearing. Thus, upon annealing (Figures 2c and 3c), the interphase morphology is retained, while the morphology of LCP molecules farther away from GF is changed from banded to tight texture.

For sample LCP/GF/ γ -MPS, a completely different interphase morphology exists (Table 2). Interfacial modification on the GF by the coupling agent must play an influential role, causing LCP molecules to lie perpendicular (by SEM) to GF. This surface force is definitely large enough to surpass the physical force provided by the GF, not to mention the mechanical force brought about by shearing; therefore the guiding, anchoring, and packing effects of GF are completely disguised. Thus, we can state

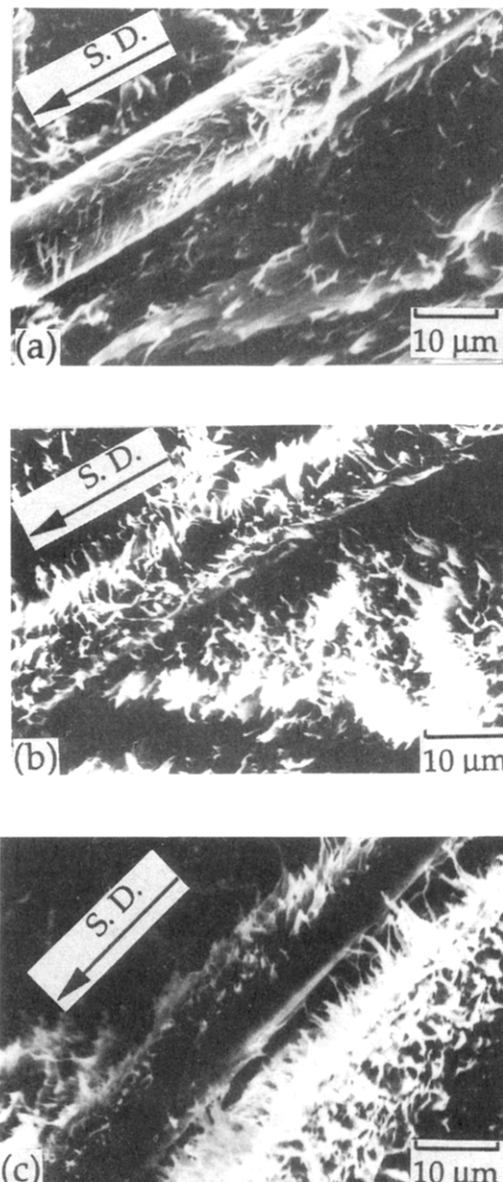


Figure 6. Scanning electron micrographs of sheared films (with high shear rate) of sample (a) LCP/GF, (b) LCP/GF/ γ -MPS, and (c) LCP/GF/PTS. Samples were cryogenically fractured.

Table 2. Molecular Orientation of LCPs by PLM^a

sample	LCP/GF		LCP/GF/ γ -MPS		LCP/GF/PTS	
	as-sheared	an-nealed	as-sheared	an-nealed	as-sheared	an-nealed
near GF	PL		PL	PP	PP	RM
	PL		RM	PL	RM	PL
away from GF						
near GF	High Shear Rate		Low Shear Rate		High Shear Rate	
	less PL	RM	PP	PP	RM	RM
away from GF	less PL		less PL		less PL	
	RM	less PL	RM	less PL	RM	RM

^a PL = parallel to glass fiber; PP = perpendicular to glass fiber; RM = random orientation.

the orientation of the LCP molecules around γ -MPS-treated GF is strongly affected by the chemical environment at the interphase.

In explaining the origin of the banded texture perpendicular to the GF for sample LCP/GF/ γ -MPS, we rule out the possibility of transcrystallization, a common phenomenon found in the Kevlar fiber-reinforced polypropylene composites and other composite systems.^{21,22} The occur-

Table 3. Summary of DSC Thermograms

sample	low-temp peak			high-temp peak		
	T _m (°C)	ΔH (J/g)	X _c (%)	T _{k-n} (°C)	ΔH (J/g)	X _c (%)
LCP						
1st scan	231	0.6	5.0	274	1.5	11.0
2nd scan				275	1.5	11.0
LCP/γ-MPS						
1st scan	224	1.6	12.0	274	0.5	4.0
2nd scan	229	0.7	5.0	276	1.2	9.0
LCP/PTS						
1st scan				273	1.5	11.0
2nd scan				276	1.4	10.0

rence of transcrystallinity in these composites was related to the crystallization conditions such as the crystallization temperature, the melt precrystallization temperature, and the residence time at precrystallization temperature. It was attributed to the presence of heterogeneities in the bulk and the preformed self-seeded nuclei located in the anfractuosity of the fiber surface. However, unlike the semicrystalline polypropylene, our LCP has a crystallinity of less than 15% (Table 3), which makes it relatively difficult to induce transcrystallinity in our study.

A more possible reason is the occurrence of transesterification between LCPs and γ -MPS. Bladon et al. reported the phenomenon of transesterification in nematic polymers,²³ a chemical process where LCP chains exchanged material at a fixed overall chain number. Transesterification between copolyesters with different polyester compositions has also been investigated using WAXD, DSC, and small-angle neutron scattering.^{24,25} Similar transesterification between LCP and γ -MPS is speculated, since there are also abundant C=O groups in the γ -MPS molecules. The transesterification we discussed here is completely different from those reported in the literature, where copolyester chains exchanged materials between similar polyester components. When γ -MPS was first brought into contact with the glass fiber, one of the methoxy groups $-\text{OCH}_3$ (becoming $-\text{OH}$ after hydrolysis) first reacted with the glass fiber to form Si—O—M chemical bonding, where M is Si, Fe, and Al in the glass fiber. This allows "standing" of γ -MPS on the GF surface. At the same time, the other two methoxy groups ($-\text{OH}$ after hydrolysis) reacted with adjacent γ -MPS molecules, also standing on the surface, to form intermolecular Si—O—Si chemical bondings.

According to Creagh and Kmetz,⁸ the γ -MPS-modified surface of the glass fiber may possess a high surface energy. This high surface energy combined with the subsequent chemical transesterification between γ -MPS and LCP molecules facilitates the LCP molecules nearby to form a perpendicular-to-GF alignment ca. 10–20 μm wide. With a high degree of registration of the LCP chains, the alignment results in the optical banded texture which is parallel to GF, as observed in PLM (Figure 4). Figure 7 illustrates the mechanism of the interaction scheme. The chemical transesterification reaction is not affected by the annealing; therefore, the annealed samples (Figure 4c,d) retained the same interphase morphology, but LCP molecules farther away from the interphase region showed a disordered microstructure. Note further that a sharp interface between the interphase layer and the bulk LCPs can be identified; we attribute this sharp interface to the high rigidity of the main-chain LCP molecules and the high shear rate applied.

In view of the persistence length of the typical LCP molecules, i.e., ca. 200 Å, a banded LCP alignment of 10–20 μm wide in the presence of γ -MPS seems too long. In

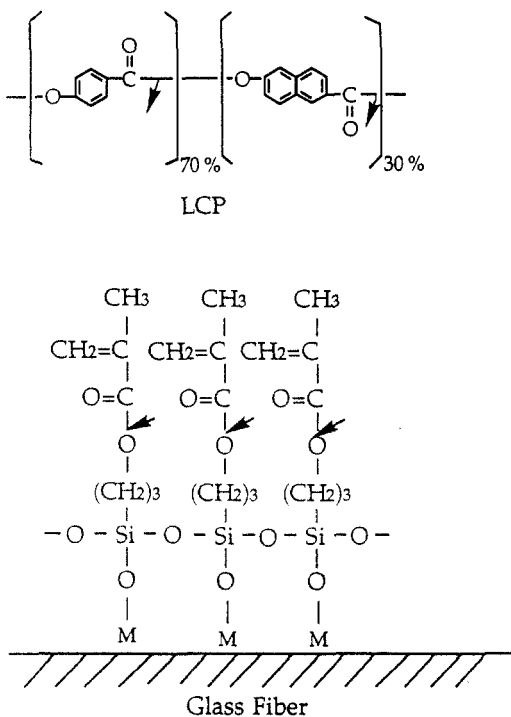


Figure 7. Proposed chemical inter-reactions among the coupling agent γ -MPS, glass fibers, and LCP.

addition to the short-range chemical transesterification, it is highly likely that there exists long-range physical factors which allows extended alignment of LCP chains. We attribute this extended alignment to the minimization of long-range elastic interaction caused by the relatively high surface energy, as suggested by Shen et al.⁹

The transesterification reaction is not expected in the case of PTS-treated composites because of its aromatic moiety, although both γ -MPS and PTS are able to interact with GF by the formation of Si—O—Si bondings. The loose interphase morphology of LCP/GF/PTS may now be rationalized. Without any chemical interaction between LCP and PTS, the PTS molecules sever only to lubricate the GF surface. The original coarse surface of GF then becomes smoother. Accordingly, the guiding, anchoring, and packing effects of GF are all disguised. From the viewpoint of adhesion, the use of PTS as the coupling agent is not recommended. On the other hand, the PTS-treated GF may result in a reduction of the anisotropization of the short fiber-reinforced LCP composites. This provides potential applications where isotropic mechanical properties of the composites are preferred.

Thermal and X-ray Diffraction Analyses of LCP/Coupling Agent. To gain some insight as to how the coupling agents affect the interphase, thermal and wide-angle X-ray diffraction analyses were further performed. Illustrated in Figure 8 are the results from thermal analyses using DSC. For the neat LCP, the first scan indicates two endothermic peaks located at 231 and 274 °C, respectively; the former is considerably smaller than the latter. The low-temperature peak disappears after the second scan, while the high-temperature peak shifts to a higher temperature and becomes broader and larger. The nature of the double endothermic peaks in this study is somewhat different from the reported melting behavior of semicrystalline polymers or polymer blends where the low-temperature peak was generally very close to the major high-temperature peak. It is also different from the

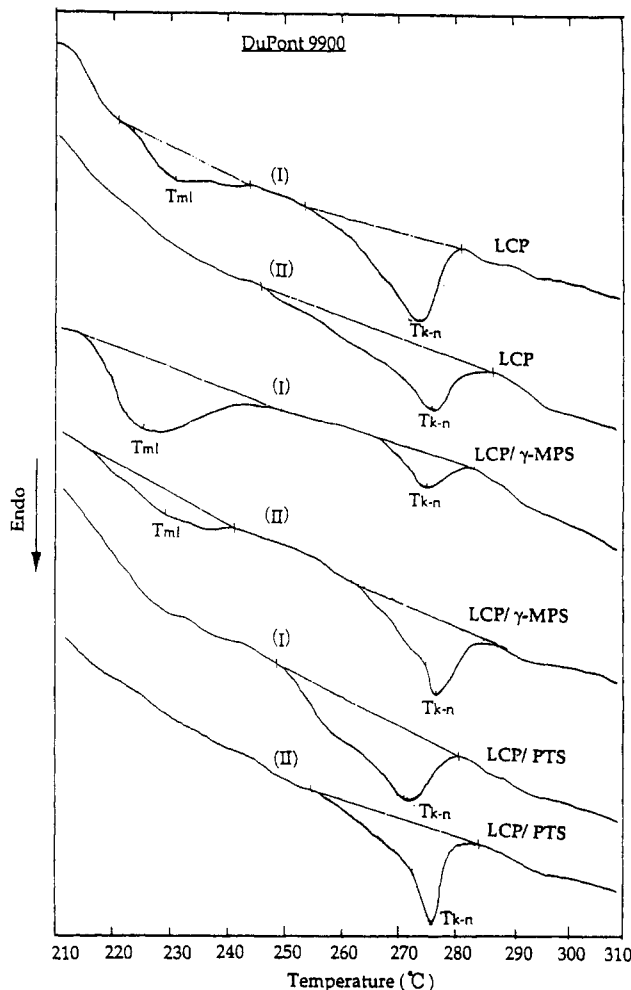


Figure 8. DSC thermograms of the first (I) and second (II) heating scans at 20 °C/min for neat LCP, LCP/γ-MPS, and LCP/PTS.

reported melting behavior of nematic copolymers where crystallization rates or annealing conditions varied.^{18,26}

The high-temperature peak indicates the melting of the high-order crystals to become nematic, i.e., the k-n transition. The existence of the low-temperature peak may be due to the previous shearing effect which allows LCP molecules to possess certain degree of local order through longitudinal motion. The degree of this local order is lower than that of the high-temperature one; it is located between the solid crystalline phase and the nematic phase. This low-temperature peak is quite unstable; therefore, it disappears during the second scan. We attribute this to the release of the shearing force after the second scan due to fast cooling.^{18,27,28} This argument is supported by the retention of the crystallinity level $X_c = 11\%$ after second heating, as listed in Table 3. Note that the crystallinity is calculated by $\Delta H_m / \Delta H_m^0$, where ΔH_m is the enthalpy of the k-n transition for the samples melted at 20 °C/min and $\Delta H_m^0 = 13.6$ J/g is the corresponding equilibrium enthalpy of the k-n transition.¹⁸

For the sample LCP/γ-MPS (Figure 8), the first DSC scan also indicates two endothermic peaks at 224 and 274 °C, respectively. Unlike the case of neat LCP, the low-temperature peak is now considerably larger than the high-temperature peak. During the second scan, these two peaks remain essentially unchanged, with only a slight shifting toward the high-temperature end, that is, 229 and 276 °C. It is interesting to note that the high-temperature peak is now larger than the low-temperature peak. The origin of this low-temperature peak may come from the

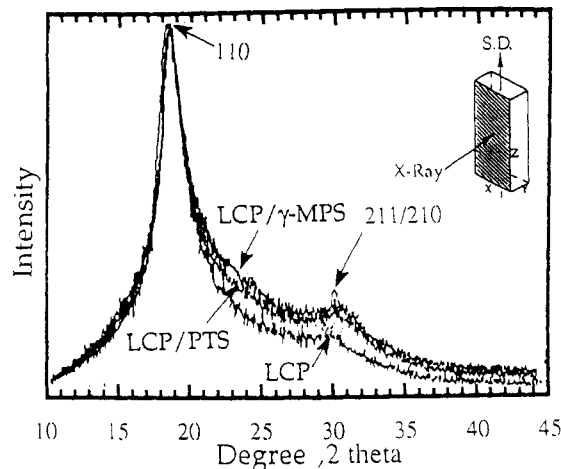


Figure 9. Wide-angle X-ray diffraction profiles of LCP, LCP/γ-MPS, and LCP/PTS, with the X-ray incident beam perpendicular to the shear direction.

transesterification between LCPs and γ-MPS and the shear-induced local order as described in the preceding section for the neat LCP sample. It is definitely not an endothermic peak due to the boiling of γ-MPS since its boiling temperature is 104 °C, far below this low-temperature peak. During the second scan, the shear-induced local order disappears and becomes part of the high-temperature peak, while the transesterification-induced crystallinity is not affected because of the chemical bondings created. This explains the broadening of the high-temperature peak and the narrowing of the low-temperature peak after the second scan. A close check of the crystallinity in Table 3 also reveals an increase (from 4 to 9%) for the high-temperature peak and a decrease (from 12 to 5%) of the low-temperature peak after the second heating.

As for the sample LCP/PTS (Figure 8), only one high-temperature peak at 273 °C with 11% crystallinity exists during the first scan; no low-temperature peak is observed (Table 3). The second scan results in a slightly higher melting temperature and a lower crystallinity, i.e., 276 °C and 10%. The local order existing in the neat LCP now is disrupted; PTS provides no opportunity for chemical reactions like transesterification but just a physical coating of the GF surface.

Generally speaking, in the presence of the coupling agents, the melting temperature of the k-n transition increases more or less during the second DSC heating (Table 3). This raises the question of whether the crystalline structure of LCP can be altered by the coupling agents. WAXD data for the DSC samples after the second scan, as illustrated in Figure 9, show no appreciable difference between the neat LCPs and those coupling agent-treated LCPs. Consistent results can be found when one compares the three DSC traces of the second scan in Figure 8, where almost the same size of the endothermic peaks are observed. This suggests the crystalline structure of LCP is almost not affected by the coupling agents used. It could possibly be due to the large difference of molecular size of the coupling agents (γ-MPS, MW = 234; PTS, MW = 226) and LCP (MW = 30 000). The LCP molecules under such circumstances assume free chain motion in the process of crystalline lattice packing. The reaction site for transesterification to occur in the case of LCP/γ-MPS is not exactly known at this point; the functional groups C=O at the chain ends of the rodlike LCP molecules are the potential sites.

Conclusions

The interphase morphology of liquid crystalline polymer/glass fiber composites has been investigated using PLM, SEM, DSC and WAXD in this study. For the composite with untreated glass fiber, a thin layer of LCP molecules ca. 10 μm with banded optical texture parallel to the glass fiber was identified. This texture remained unaffected by subsequent annealing at 320 °C for 60 min. Formation of this interphase morphology was attributed to the guiding, anchoring, and packing effects of GF. These effects were greater than the mechanical shearing effect. For the composite with γ -MPS-treated GF, the same thin layer of LCP molecules ca. 10–20 μm wide with also the banded texture was identified; it was perpendicular to GF and was not affected by annealing. It was attributed to the occurrence of transesterification between LCP molecules and γ -MPS which provided a high-energy GF surface, facilitating the LCP molecules nearby to form a perpendicular alignment. For the composite with PTS-treated GF, a loose or random arrangement of LCP molecules of ca. 5 μm was found. The coupling agent PTS served only to lubricate the GF surface; thus all the effects brought about from GF were disguised. Existence of the endothermic transition at 224 °C further supported the proposed transesterification reaction; this transition was not affected by the second DSC scan but just became smaller. WAXD results indicated that the crystalline structure of LCP was almost not affected in the presence of the coupling agent. This could be due to the large difference in molecular size of the LCP and the coupling agent.

Acknowledgment. This research work is sponsored by the National Science Council, Taiwan (Contract No. NSC 82-0405-E-110-097). Material donation from Professor H. T. Chiu at the National Taiwan Institute of Technology is highly appreciated.

References and Notes

- (1) Chung, T. S. *Polym. Eng. Sci.* 1986, 26, 901.
- (2) Chung, T. S.; McMahon, P. E. *J. Appl. Polym. Sci.* 1986, 31, 965.
- (3) Voss, H.; Friedrich, K. *J. Mater. Sci.* 1986, 21, 2889.
- (4) Chivers, R. A.; Moore, D. R. *Polymer* 1991, 32, 2190.
- (5) King, J. A.; Buttry, D. A.; Adams, D. F. *Polym. Compos.* 1993, 14, 292.
- (6) King, J. A.; Buttry, D. A.; Adams, D. F. *Polym. Compos.* 1993, 14, 301.
- (7) Bhama, S.; Stupp, S. I. *Polym. Eng. Sci.* 1990, 30, 228.
- (8) Creagh, L. T.; Kmetz, A. R. *Mol. Cryst. Liq. Cryst.* 1973, 24, 59.
- (9) Shen, Y. R.; Chen, W.; Feller, M. B.; Huang, J. Y.; Superfine, R. *Mol. Cryst. Liq. Cryst.* 1991, 207, 77.
- (10) Shieh, J. J.; Hsu, T. J. *Polym. Eng. Sci.* 1992, 32, 335.
- (11) Viney, C.; Donald, A. M.; Windle, A. H. *J. Mater. Sci.* 1983, 18, 1136.
- (12) Kléman, M.; Liébert, L.; Strzelecki, L. *Polymer* 1983, 24, 295.
- (13) Thomas, E. L.; Wood, B. A. *Faraday Discuss. Chem. Soc.* 1985, 79, 229.
- (14) Bedford, S. E.; Windle, A. H. *Polymer* 1990, 31, 616.
- (15) Donald, A. M.; Windle, A. H. *J. Mater. Sci.* 1983, 18, 1143.
- (16) Viney, C.; Donald, A. M.; Windle, A. H. *Polymer* 1985, 26, 870.
- (17) Chen, S.; Jin, Y.; Xu, M. *Polym. Commun.* 1987, 28, 208.
- (18) Kamal, M. R.; Khennache, O.; Goyal, S. K. *Polym. Eng. Sci.* 1989, 29, 1089.
- (19) Romo-Uribe, A.; Windle, A. H. *Macromolecules* 1993, 26, 7100.
- (20) Viney, C.; Mitchell, G. R.; Windle, A. H. *Polym. Commun.* 1983, 24, 145.
- (21) Avella, M.; Della-Volpe, G.; Martuscelli, E.; Raimo, M. *Polym. Eng. Sci.* 1992, 32, 376.
- (22) Avella, M.; Della-Volpe, G.; Martuscelli, E.; Raimo, M. *Polym. Eng. Sci.* 1992, 32, 383.
- (23) Bladon, P.; Warner, M.; Gates, M. E. *Macromolecules* 1993, 26, 4499.
- (24) MacDonald, W. A.; McLenaghan, A. D. W.; McLean, G.; Richards, R. W.; King, S. M. *Macromolecules* 1991, 24, 6164.
- (25) McCullagh, C. M.; Blackwell, J.; Jamieson, A. M. *Macromolecules* 1994, 27, 2996.
- (26) Butzbach, G. D.; Wendorff, J. H.; Zimmermann, H. J. *Polymer* 1986, 27, 1337.
- (27) Lin, Y. G.; Winter, H. H. *Macromolecules* 1988, 21, 2439.
- (28) Lin, Y. G.; Winter, H. H. *Macromolecules* 1991, 24, 2877.